Fuel Cells DOI: 10.1002/fuce.200900062

Synthesis of Poly (2,2′-(1,4-phenylene) 5,5′-bibenzimidazole) (*para*-PBI) and Phosphoric Acid Doped Membrane for Fuel Cells▲

S. Yu[1,a], H. Zhang[1,b], L. Xiao[1,c], E.-W. Choe[1], and B. C. Benicewicz[1]*

[1] Department of Chemistry and Biochemistry, USC NanoCenter, University of South Carolina, Columbia, SC 29208, USA

Received March 27, 2009; accepted April 3, 2009

Abstract

A detailed investigation of the polymerisation conditions for poly(2,2′-(1,4-phenylene)5,5′-bibenzimidazole) (*para*-PBI) in polyphosphoric acid (PPA) led to the preparation of high molecular weight polymer. The polymer solutions could be used directly to produce phosphoric acid (PA)-doped PBI membranes by the PPA process. These membranes showed very high PA doping levels, i.e., up to ~30 moles of PA per mole of PBI repeat unit. The ionic conductivity of the membranes was 0.24 S cm^{-1} at 160 °C. Fuel cell performance was measured at various operating conditions by changing temperature, pressure and gases and verified the high carbon monoxide (CO) tolerance of fuel cells operating at this temperature.

Keywords: High Temperature Polymer Electrolyte Membrane (PEM), para-PBI Polymerisation, Phosphoric Acid Doped Membrane, PBA Process, Proton Conductivity, Polybenzimidazole

1 Introduction

Recently, a new generation of proton exchange membrane (PEM) fuel cells based on PA-doped polybenzimidazoles (PBI) electrolyte membranes have received attention for the distinct differences over the traditional perflouorsulfonic acid (PFSA) polymer electrolyte membrane fuel cells [1–7]. These advantages include the high temperature of operation (up to 200 °C), ability to operate without humidified feed streams, and increased tolerance to CO. The published PBI candidates for fuel cell membranes are still limited to few chemical structures, including poly(2,2′-(*m*-phenylene)-5,5′-bibenzimidazole) (*meta*-PBI), poly(2,5-benzimidazole) (ABPBI) and poly(2,2′-(2,6 (or 3,5)-pyridine)-5,5′-bibenzimidazole). Among the different structures, *meta*-PBI is the most commonly studied and was commercialised by Celanese Corporation in the 1980s for use mainly as a high temperature resistant fibre and fabric. A large number papers and reviews are available which describe the history, synthesis, processing, properties and applications of fibres based on *meta*-PBI [8–12].

In contrast, there are very limited reports on the more rigid *para*-oriented PBIs. Vogel and Marvel prepared some *para*-oriented PBIs in the original work on aromatic PBIs by a melt/solid state polymerisation process [13]. Korshak et al. also prepared some *N*-phenylated *para*-oriented PBIs [14]. Based on inherent viscosity (I. V.) measurements in this work, it appears that relatively low molecular weight polymers were obtained by these early polymerisation attempts. Polymerisations conducted by Iwakura et al. [15] and Varma and Veena [16] used 3,3′,4,4′-tetraaminobiphenyl tetrachloride with the

▲ *Paper presented at the MEA'08 Conference, La Grande Motte, 21st–24th September 2008.*

[a] *Current address: BASF Fuel Cell, Inc., 39 Veronica Ave, Somerset, NJ 08873, USA*

[b] *Current address: Hollingsworth & Vose, 5035 County Route 113, Easton, NY 12834, USA*

[c] *Current address: Pall Corporation, 25 Harbor Park Drive North, Port Washington, NY 11050, USA*

[*] *Corresponding author, benice@sc.edu*

free diacids or their derivatives in polyphosphoric acid (PPA) to obtain slightly higher I.V. polymers. Subsequent development work sponsored by the US Air Force Materials Lab [17, 18] resulted in *para*-oriented PBI polymers with high I.V., although in some instances the polymerisations required almost five weeks of heating during the polymerisation due to the lengthy dissolution time for terephthalic acid (TA) in PPA. The low solubility of TA in PPA, approximately 0.0006 g in 1 g of PPA (86 wt.-% P_2O_5) at 140 °C, and its effects on the polymerisation of rigid-rod polymers were reported in elegant work by So et al. [19–21] Thus, it appears that the low solubility of TA and the *para*-oriented PBIs limited the development of appropriate synthetic conditions for the preparation of high molecular weight polymers. Additionally, the early work on high performance fibres focused on polybenzoxazole (PBO) and polybenzthiazole (PBZT) polymers because of their solubility at higher concentrations and access to lyotropic liquid crystalline phases at these higher concentrations. The challenges of synthesizing and processing *para*-oriented PBIs have been cited as the main reasons for the lesser attention given to these polymers, and the subsequent development and commercialisation of *meta*-PBI as a commercial fibre and fabric [9, 10, 12].

Recently, we reported on a new sol–gel process to prepare high PA-doped *para*-oriented PBI polymer membranes from PPA solutions [5]. The new process provided some clear advantages in the processing and preparation of PA-doped PBI membranes. NMR studies on PA-doped *meta*-PBI membranes prepared by both the conventional imbibing process and the new PPA process showed fundamental differences in the transport properties of the resulting membranes [22]. In the present paper, we describe the detailed synthetic procedures for the preparation of high molecular weight *para*-PBI, characterisation of the PA-doped membranes and the performance of these membranes in high temperature fuel cells.

2 Experimental

Chemicals. 3,3′,4,4′-tetraaminobiphenyl (TAB, 97%) was used as received from Celanese Ventures, GmbH. Terephthalic acid (TA, polymerisation grade) was purchased from Amoco Chemical Company. Polyphosphoric acid (PPA) was purchased from Aldrich Chemical Corporation.

para-PBI Membrane Preparation. 3,3′,4,4′-Tetraaminobiphenyl (TAB), terephthalic acid (TA) and polyphosphoric acid (PPA) were put in a three-neck flask equipped with a nitrogen flow and overhead mechanical stirrer (Figure 1). The solution was stirred for 3 h at 140 °C and heated to 195–220 °C (maintained for 20 h at the various polymerisation temperatures) for polymerisation. The monomer concentration and temperature profile (final polymerisation temperature) were changed to investigate the effects of the polymerisation variables on polymer I.V. When polymerisation was complete, 85% *o*-phosphoric acid (PA) was added to dilute the solution if the solution viscosity was too high to cast membranes using a Gardner blade. The *para*-PBI membrane used for fuel cell testing was prepared by the following procedure: TAB (8.160 g, 38.08 mmol), TA (6.327 g, 38.08 mmol) and 115% polyphosphoric acid (400 g) were placed in a 500 mL round bottom flask equipped with an overhead stirrer and nitrogen inlet. The solution temperature was controlled using an oil bath equipped with an automatic temperature controller. The solution was stirred at 140 °C for 3 h and at 195 °C for 13 h. After polymerisation, the solution temperature was increased to the casting temperature, 220 °C and 35 mL of 85% *o*-phosphoric acid was added to adjust the solution viscosity for membrane casting. A small amount of the polymer solution was removed, precipitated in water, neutralised with ammonium hydroxide, and vacuum dried at 120 °C to isolate the polymer powder. The I. V. of the polymer in 96% sulfuric acid (30.0 °C) at a concentration of 0.2 g dL^{-1} was 3.5 dL g^{-1}. After polymerisation, the hot polymer solution in polyphosphoric acid was poured on a glass plate for casting using a Gardner blade at the gate thickness of 500 µm. PA-doped *para*-PBI gel membrane was obtained by hydrolysing in a humidity controlled chamber at 40% relative humidity (RH), 27 ± 1 °C for 24 h as reported previously [4, 5]. The final membrane thickness after hydrolysis was approximately 400 µm. The isolated p-PBI polymer was analysed by FTIR, NMR and thermal analysis. The FTIR spectrum showed a N-H stretching peak at 3,415 cm^{-1}, and peaks in the range of 1,650–1,500 cm^{-1} consistent with the benzimidazole rings. Broad peaks at 1,250–750 and 500 cm^{-1} were not seen, which would have been representative of PA still remaining in the washed sample. Proton NMR (in D_2SO_4) showed peaks at 8.45, 8.25, 7.98 and 7.84 ppm for the aromatic protons. Thermal analysis did not show any peaks in the DSC, and TGA scans indicated the decomposition started at approximately 550 °C.

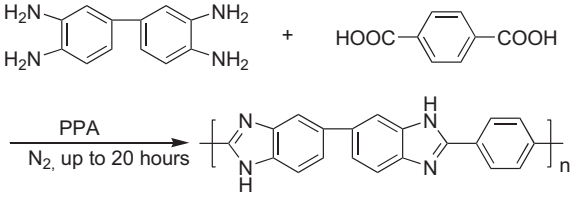

Fig. 1 Synthetic scheme for the synthesis of *para*-PBI in polyphosphoric acid (PPA).

General Measurements. For the membrane composition measurements, the acid content in the membrane was determined by titration on pre-weighed samples. Three pieces of membrane sample were titrated with a standardised 0.1 N sodium hydroxide solution using a Metrohm 716 DMS Titrino titrator. The dry weight of polymer was obtained by washing the samples with water, and then drying in a vacuum oven overnight at 160 °C. The remaining weight in the acid doped membrane, after subtracting the weight of polymer and phosphoric acid, was assumed to be water only. The PA doping level, X, reported as moles of phosphoric acid per PBI repeat unit (PBI·XH_3PO_4) was calculated from the Eq. (1)

$$\text{PA doping level X per PBI unit} = \frac{(V_{NaOH} \times C_{NaOH})}{(W_{dry}/M_w)} / \qquad (1)$$

where V_{NaOH} and C_{NaOH} are the volume and the molar concentration of the sodium hydroxide titer, while W_{dry} is the dry polymer weight and *M*w is the molecular weight of the polymer repeat unit, respectively.

The ionic conductivity through the membrane was measured by a four-probe AC impedance method using a Zahner IM6e electrochemical station in the frequency range of 1 Hz to 100 KHz at temperatures from room temperature to 180 °C. A rectangular piece of membrane (3.5 × 7.0 cm^2) in a four-probe impedance cell was placed into a programmable oven to measure the membrane conductivity at different temperatures from 20 to 180 °C at steps of 20 °C in dry conditions.

Fuel Cell Testing. Single cells with 45.15 cm^2 of active area were used to measure the performance of PA-doped PBI based PEM fuel cells. PA-doped PBI gel membranes prepared as described earlier [4, 5] were placed between the anode and cathode electrodes, and hot-pressed at 140 °C for 30 s to fabricate membrane electrode assemblies (MEA). Gas diffusion electrodes were obtained from E-TEK, Inc. with 30% Pt/C catalyst (1 mg cm^{-2} on carbon, Vulcan XC-72) for both anode and cathode. The polarisation curves were obtained by both constant gas stoichiometry (λ) and constant gas flow rate methods under various fuel cell operating temperatures, gas pressures and gas compositions. Two compositions of mixed gases were used to simulate hydrogen containing reformed fuels from natural gas (hydrogen 35.8%, carbon monoxide 0.2%, carbon dioxide 11.9% and nitrogen balance) and methanol (hydrogen 70%, carbon monoxide, 1.0% and carbon dioxide balance). The fuel and oxidant gases were supplied without humidification.

3 Results and Discussion

Synthesis of para-PBI. High molecular weight poly(2,2′-(1,4-phenylene)5,5′-bibenzimidazole) (*para*-PBI) was obtained by polymerizing equimolar amounts of 3,3′,4,4′-tetraaminobiphenyl and terephthalic acid in polyphosphoric acid under nitrogen purging. The effects of monomer concentration and temperature profile were the main variables used to investigate the polymerisation conditions. Figure 2 shows the isolated effect of monomer concentration on the polymer I. V. by fixing the final polymerisation temperature at 195 °C for 20 h. Each data point in Figure 2 represents a polymerisation conducted at a 1 L scale. I.V. of the polymers increased with increase in the monomer concentration in polyphosphoric acid solution up to 4.5 wt.-% of monomer concentration and decreased abruptly at higher monomer concentrations. The initial increase in I.V. with increase in the monomer concentration is easily explained by the normal dependence of the polymerisation rate with monomer concentration. However, there was a maximum I. V. (~3.0 dL g^{-1}) point at the monomer concentration of nearly 4.5 wt.-% in PPA solution. At monomer concentrations above this value, the polymer solution became so viscous during the early stages of the polymerisation that efficient stirring could not be maintained at these monomer concentrations and limited the mobility of chain ends to react and complete the polymerisation. This is likely to be the cause for lower and unpredictable I.V. values at higher monomer concentrations.

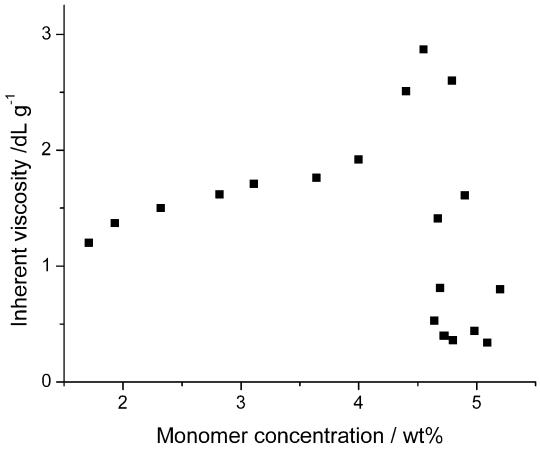

Fig. 2 Effect of monomer concentration on the *para*-PBI inherent viscosity (I.V.) at a polymerisation temperature of 195 °C.

Higher final polymerisation temperatures (220 °C) were also investigated. At high temperatures, the viscosity of the solution was lowered and allowed the polymerisation to continue with efficient stirring even at moderate monomer concentrations. Table 1 shows the I.V. results for polymerisations conducted at nearly equivalent monomer concentration at two different final polymerisation temperatures. The higher polymerisation temperature and the ability to conduct the polymerisation without loss of stirring clearly led to higher I.V.s and homogeneous solutions. An I.V. of 3.8 dL g^{-1} was obtained at 3.0 wt.-% monomer concentration when the polymerisation was conducted at 220 °C. *Para*-PBI of high molecular weight has negligible solubility in organic solvents and cannot be processed by dissolving and casting in organic solvents to obtain membranes for fuel cell applications. Only low molecular weight *para*-PBI and PBIs of different chemical structures which exhibit higher solubilities can be processed into membranes using organic solvents. Membranes obtained by such processes are subsequently doped with phosphoric acid by soaking in phosphoric acid baths. In this work, the PPA/polymer solution was directly cast to prepare high

Table 1 Effect of polymerisation temperature for the synthesis of p-PBI[a]

Monomer concentration (wt.-%)	Polymerisation temperature (°C)	Inherent viscosity (dL g^{-1})
1.0	220	2.5
1.9	195	1.4
2.0	220	3.0
2.3	195	1.5
2.5	220	3.1
3.1	195	1.7
3.0	220	3.8

(a) Polymerisations conducted by heating for 3 h at 140 °C, and for 20 h at the final polymerisation temperature indicated above.

PA-doped membranes by the PPA process as described earlier [4, 5]. After direct casting of the polymer solution onto glass plates, samples were placed in a controlled humidity chamber for 24 h. The PPA/polymer solution absorbed moisture from the environment, which led to PPA hydrolysis and the formation of PA *in situ*. The cast film was transformed into a gel membrane, and some water and PA were observed to drain from the film. The membrane composition was determined by titrating membrane pieces with 0.1 N NaOH solution when the membrane hydrolysis was conducted at 40% RH for more than 40 h. Figure 3 shows the effect of hydrolysis time after casting on the membrane composition. Water absorption and PPA hydrolysis occurred rapidly within the initial 4 h of exposure to a humidified environment. The membrane composition at 23.5 h after casting was 68.44 wt.-% of phosphoric acid, 25.00 wt.-% of water and 6.56 wt.-% of polymer. This corresponds to doping level of 31.8 moles of PA per mole of PBI repeat unit. For comparison, the maximum doping level reported in the literature by immersing the dry film in the PA solution was 13–16 moles of acid per polymer repeat unit for *meta*-PBI [22, 23]. The *para*-PBI membranes prepared by the PPA sol–gel method achieved high acid doping levels in this relatively simple process.

3.1 *para*-PBI/PA Membrane Properties

Ionic conductivity. Figure 4 shows the ionic conductivity of the PA-doped *para*-PBI membrane at different temperatures. All the measurements were conducted without any environmental control except temperature. The ionic conductivity of the membrane was measured three times to analyse the effects of changes in the membrane composition (*via* water evaporation) during the heating process. The top curve (squares) in Figure 4 was the initial run, which measured the membrane conductivity without any pre-treatment. Thus, the membrane at this stage of testing contained phosphoric acid,

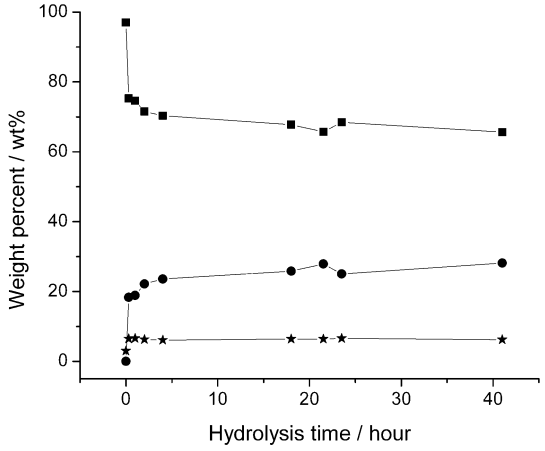

Fig. 3 The change in phosphoric acid doped *para*-PBI membrane composition (squares, phosphoric acid; circles, water; stars, *para*-PBI) with time when hydrolysed at 25 °C, 40% RH.

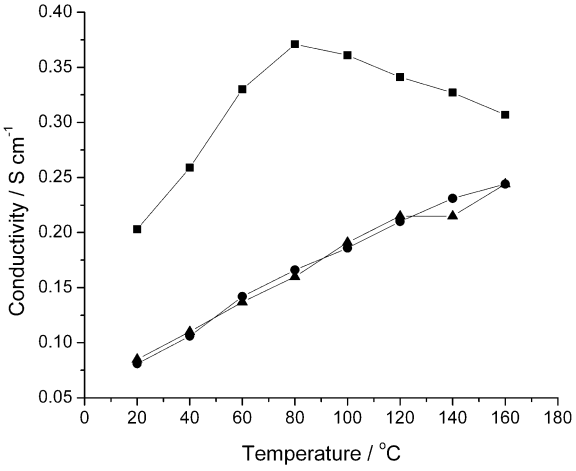

Fig. 4 Effects of temperature on ionic conductivity for PA-doped *para*-PBI membrane (squares, 1st run; circles, 2nd run; triangles, 3rd run).

water and polymer. Because the membrane contained a large amount of water, both the membrane composition and membrane dimensions changed during the test as the temperature was increased to 160 °C and water content decreased. In the first run, the conductivity increased with increase in temperature until approximately 80 °C. At temperatures of 80–100 °C, water began to be removed from the membrane and this effect dominated the conductivity behaviour. The conductivity-temperature curve showed a peak at 80 °C in the first conductivity measurement when a large amount of water was still present in the membrane. It should be noted that, initially, both water and PA contributed to the experimentally measured ionic conductivity. When the temperature was greater than 80–100 °C, the water loss continued and caused the conductivity to decrease. This phenomenon is the same as in all water dominated proton exchange membranes such as Nafion [24]. Water loss also caused dimensional changes. To obtain reliable data, the second and third membrane conductivity tests were performed using corrected sample dimensions. The sample dimensions and conductivity were identical in the second and third conductivity tests. In the second and third tests, after removal of the free water, the membrane conductivity increased uniformly with temperature. The conductivity, 0.24 S cm^{-1} at 160 °C, is higher than previously published data, which is typically 0.1–0.13 S cm^{-1} at 160 °C [25] for *meta*-PBI. This is mainly due to the high acid content in the gel membrane. However, previous NMR studies also showed that the membrane preparation process and resulting physical structure also significantly affect proton transport properties [26].

The long-term stability of the ionic conductivity was also evaluated by placing the membrane in the conductivity cell and heating quickly to 180 °C, followed by continued heating at this temperature while measuring the conductivity as a function of time. The results are shown in Figure 5 which shows both the temperature profile and conductivity measurements. The initial increase in the conductivity represents

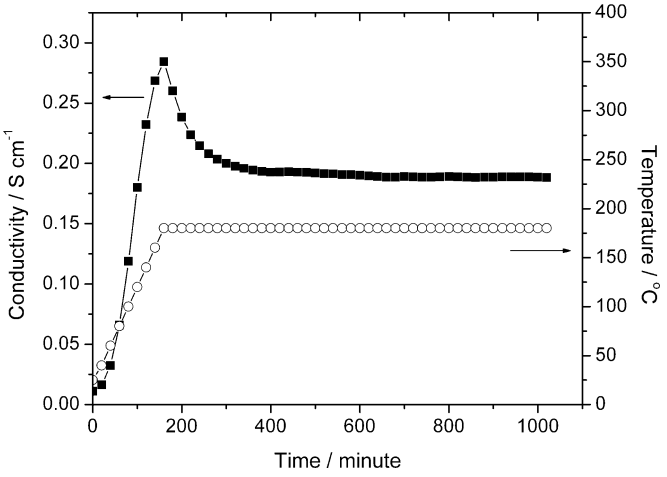

Fig. 5 Long-term conductivity measurements at 180 °C for *para*-PBI/PA membrane.

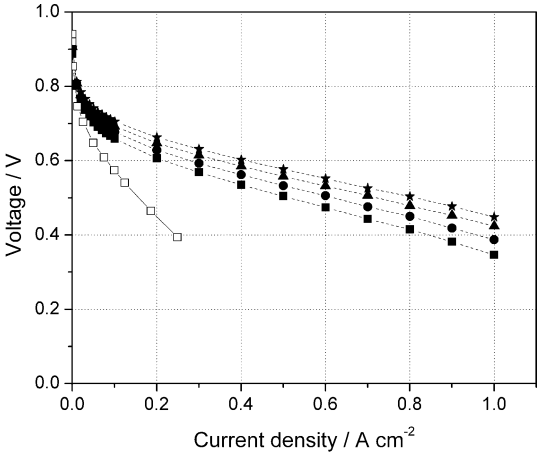

Fig. 6 Polarisation curves *para*-PBI membrane based fuel cells with hydrogen (λ = 1.2)/air (λ = 2.00) at different temperatures and at ambient pressure (1 atm, absolute) by constant stoic mode. (Squares: 120 °C, circles: 140 °C, triangles: 160 °C and stars: 180 °C). Open squares are data from reference [2] on PA doped m-PBI at 150 °C.

the effects of higher temperatures when both phosphoric acid and water were present in the film. As discussed previously, the water will be driven out the membrane at temperatures above approximately 80–100 °C and cause a decrease in conductivity which was observed dynamically in this study. A constant conductivity was observed after approximately 250 min. This suggests that the loss of additional water from the condensation of phosphoric acid molecules occurs early during the heating process, and thus the acid strength of the phosphoric acid remains relatively constant at constant temperature.

Fuel Cell Testing. Fuel cell testing of PA-doped PBI membranes was conducted using 50 cm^2 single stack fuel cells (active area: 45.15 cm^2) as described in the Experimental section. Fuel cells were operated with various conditions by changing the temperature of operation, gas composition and gas pressure. Unlike conventional low temperature perfluorosulphonic acid-based or hydrocarbon-based membrane fuel cells, *para*-PBI membrane based fuel cells prepared in this work were operated without any gas humidification. Figure 6 shows the fuel cell polarisation curves of *para*-PBI based fuel cells at different temperatures with hydrogen and air. The cell voltage at 0.2 A cm^{-2} increased from 0.606 V at 120 °C to 0.663 V at 180 °C. In most PEM fuel cells, water molecules play a critical role to transport protons from the anode side to the cathode side. As a result, they require gas humidification to prevent membrane dry out, and at temperatures higher than 100 °C, gas humidification systems become more complicated to pressurise the gases and maintain water vapour pressure. Figure 6 demonstrates that phosphoric acid doped *para*-PBI based membranes can be used up to 180 °C without gas humidification due to the involvement of phosphoric acid in the proton conduction mechanism. Theoretically, the reversible cell voltage of fuel cells decreases by 0.27 mV°C^{-1} under standard conditions with H_2 and O_2 [24]. However, the empirical relationship between operating temperature and the fuel cell voltage gain (ΔV_T) of PAFCs operating at a current density of ~0.25 A cm^{-2} with hydrogen and air in the temperature region of 180 °C ≤T ≤250 °C is given by

$$\Delta V_T = 1.15(T_2 - T_1)\text{mV} \quad (2)$$

From the data in Figure 6, the dependence of the fuel cell voltage on operating temperature at 0.2 A cm^{-2} with hydrogen and air was estimated at 0.8–1.1 mV °C^{-1}. Considering the differences in detailed operating conditions, this is in reasonably good agreement with values of the more thoroughly studied PAFC system (1.15 mV °C^{-1}). The effects of other gas mixtures on fuel cell voltage are shown in Figures 7 and 8.

One of the most important advantages of high temperature PEM fuel cells is the high tolerance to impurities in the fuel gas, especially carbon monoxide [27]. In this work, fuel cell

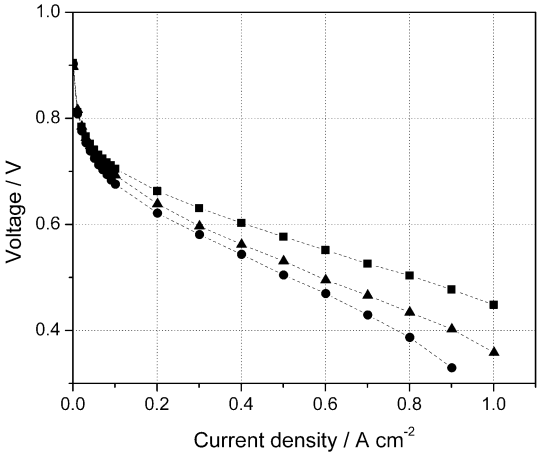

Fig. 7 Polarisation curves of *para*-PBI membrane based fuel cells with hydrogen/air and reformate/air at 180 °C under ambient pressure. [Squares: hydrogen/air, triangles: (reformate composition I, H_2 70%, CO 1%, CO_2 balance)/air and circles: (reformate composition II, H_2 35.8%, CO 0.2%, CO_2 11.9%, N_2 balance)/air by constant stoic mode, fuel (λ = 1.2)/air (λ = 2.0)].

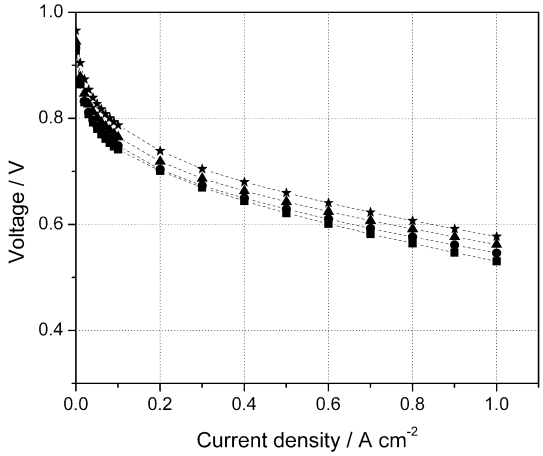

Fig. 8 Polarisation curves of *para*-PBI membrane based fuel cells with hydrogen (λ = 1.2)/oxygen (λ = 2.00) at different temperatures under ambient pressure by constant stoic mode. (Squares: 120 °C, circles: 140 °C, triangles: 160 °C and stars: 180 °C).

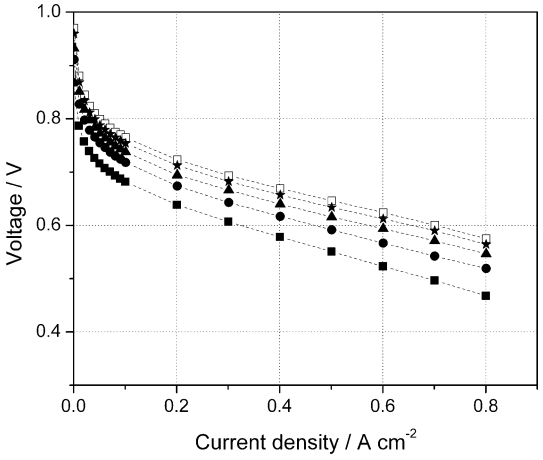

Fig. 9 Polarisation curves of *para*-PBI membrane based fuel cells with hydrogen (415 mL min^{-1})/air (1,655 mL min^{-1}) at 160 °C under different gas pressure. (Filled squares,1 atm; filled circles, 1.5 atm; filled triangles, 2 atm; filled stars, 2.5 atm; and unfilled squares, 3 atm; absolute pressures).

performance was measured with three types of fuel gases: pure hydrogen and two different compositions of reformate (composition I (H_2 70.0%, CO 1.0% and CO_2 balance) and composition II (H_2 35.8%, CO 0.2%, CO_2 11.9% and N_2 balance)). Figure 7 shows the polarisation curves at 180 °C with the different fuel gases. As compared to pure hydrogen, the fuel cell voltage at 0.2 A cm^{-2} decreased 24 mV when the gas was switched to composition I and 42 mV when the gas was switched to composition II. These decreases result from both fuel dilution and carbon monoxide (CO) poisoning of the Pt catalyst. Nonetheless, the cells were able to operate reliably on both gas compositions which mimic methanol (composition I) and natural gas (composition II) reformates. When the cell temperature was decreased to 80 °C, the fuel cell voltage at 0.2 A cm^{-2} quickly dropped to 0 V with both gases. A traditional low temperature PEM fuel cannot operate using fuels with CO concentrations of 0.2% because small amounts of carbon monoxide (5–50 ppm) poison the catalyst at the normal operating temperature (~80 °C). The oxidant composition will also affect the cathode and overall fuel cell performance. In our experiments, air and pure oxygen were used as oxidants. Because air contains approximately 21% of oxygen, the cell performance was improved due to the increase in oxygen partial pressure when oxygen was used instead of air. The fuel cell voltage gain measured when switching from air to oxygen was in the range of 54–76 mV at 0.2 A cm^{-2} as shown in Figure 8. The empirical value of the oxygen gain (191 °C, 0.3 A cm^{-2}, 1 atm) for PAFCs was ~60 mV [24]. Thus, despite the difference in operating conditions, the relationship between fuel cell voltage gain and the oxygen partial pressure was in reasonable agreement with that of PAFCs.

Figure 9 shows fuel cell performance of *para*-PBI membranes operating at different pressures at 160 °C. Gases were supplied using a constant flow rate mode due to the equipment limitation for pressurised gas operation. Gas flow rates were 415 mL min^{-1} for H_2 and 1,655 mL min^{-1} for air, which correspond to flow rates of H_2 (λ = 1.2) and air (λ = 2.0) at 1.1 A cm^{-2}. When the voltage gain at constant temperature is expressed as follows

$$\Delta V_{\text{gain}} = C \log\left(\frac{P_2}{P_1}\right) \tag{3}$$

the experimentally determined C value for a phosphoric acid fuel cell was 146 mV in the temperature range of 177 °C < T < 218 °C and pressure range of 1 atm < P <10 atm. C values calculated from Figure 9 at 180 °C, 0.2 A cm^{-2} were 176–198 mV, which means there was a greater effect of cell pressure on voltage for the *para*-PBI based fuel cells operated at 160 °C than phosphoric acid based fuel cells.

Fuel cell lifetime is one of the primary concerns in the fuel cell field as the technology progresses from the lab to real world application. For some applications, stable long-term operation under low relative humidity conditions is desirable. Our previous work on *para*-PBI membranes fabricated from the PPA process demonstrated that long-term operation for a phosphoric acid doped PBI based fuel cell at 160 °C under a variety of simulated real world environments was possible with low degradation rates and low phosphoric acid loss rates [5, 28]. Thus, it appears that PBI membrane fuel cells can be operated at a wide range of temperatures (100–200 °C) and operating conditions and could be applicable in many applications.

4 Summary and Conclusions

A thorough investigation of the polymerisation conditions for *para*-PBI was conducted. Despite the historical reports on the low solubility of *para*-PBI, the investigation of the polymerisation conditions in PPA produced high molecular

weight *para*-PBI under convenient conditions as indicated by I.V. measurements. Novel membranes were prepared by directly casting the polymerisation solution, and subsequent *in situ* hydrolysis of PPA to PA. These membranes showed extremely high acid doping levels, typically containing 3–6 wt.-% polymer, and 30–40 moles of phosphoric acid per mole of PBI repeat unit. The ionic conductivity for a *para*-PBI membrane made by this process was 0.24 S cm^{-1} at 160 °C after removal of water initially presented in the membrane. The high ionic conductivity values were reproducible upon subsequent heating cycles. Membrane electrode assemblies were fabricated from the membranes and tested in fuel cells. Extensive fuel testing of the *para*-PBI membranes was conducted, and included varying temperatures, fuel sources (both pure hydrogen and synthetic reformates with 0.2 and 1.0% carbon monoxide) and pressures. Fuel cells based on this membrane showed excellent performance and minimal CO poisoning effects when operating at high temperatures. Humidification of the gas streams was not necessary for fuel cell operation, and long-term durability in operating fuel cells is expected.

Acknowledgments

The authors gratefully acknowledge financial and technical support for this research by BASF Fuel Cell, Inc.

References

[1] R. Savinell, E. Yeager, D. Tryk, U. Landau, J. Wainright, D. Weng, K. Lux, M. Litt, C. Rogers, *J. Electrochem. Soc*. **1994**, *141*, L46.
[2] J. T. Wang, R. F. Savinell, J. Wainright, M. Litt, H. Yu, *Electrochim. Acta* **1996**, *41*, 193.
[3] Q. Li, H. A. Hjuler, N. J. Bjerrum, *J. Appl. Electrochem*. **2001**, *31*, 773.
[4] L. Xiao, H. Zhang, T. Jana, E. Scanlon, R. Chen, E. W. Choe, L. S. Ramanathan, S. Yu, B. C. Benicewicz, *Fuel Cells* **2005**, *5*, 287.
[5] L. Xiao, H. Zhang, E. Scanlon, L. S. Ramanathan, E. W. Choe, D. Rogers, T. Apple, B. C. Benicewicz, *Chem. Mater*. **2005**, *17*, 5328.
[6] J. Mader, L. Xiao, T. J. Schmidt, B. C. Benicewicz, *Adv. Polym. Sci*. **2008**, *216*, 63.
[7] D. J. Jones, J. Roziere, *Adv. Polym. Sci*. **2008**, *215*, 219.
[8] E. J. Powers, G. A. Serad, *High Perform. Polym., Proc. Symp*. **1986**, 355.
[9] A. Buckley, D. E. Stuetz, G. A. Serad, *Encycl. Polym. Sci. Eng*. **1987**, *11*, 572.
[10] E.-W. Choe, D. D. Choe in *Polymeric Materials Encyclo.*, (Eds Salamone, J.), CRC Press: New York, **1996**, Vol. 7, pp 5619-5638.
[11] T.-S. Chung, *Plast. Eng*. **1997**, *41*, 701.
[12] T.-S. Chung, *J. Macromol. Sci., Rev. Macromol. Chem. Phys*. **1997**, *C37*, 277.
[13] H. Vogel, C. S. Marvel, *J. Polym. Sci*. **1961**, *50*, 511.
[14] V. V. Korshak, A. L. Rusanov, D. S. Tugushi, G. M. Cherkasova, *Macromolecules* **1972**, *5*, 807.
[15] Y. Iwakura, K. Uno, Y. Imai, *J. Polym. Sci., Part A: Polym. Chem*. **1964**, *2*, 2605.
[16] I. K. Varma, Veena, *J. Polym. Sci., Polym. Chem. Ed*. **1976**, *14*, 973.
[17] C. B. Delano, R. R. Doyle, R. J. Miligan, AFML-TR-74-22 **1974**.
[18] R. F. Kovar, F. E. Arnold, *J. Polym. Sci., Polym. Chem. Ed*. **1976**, *14*, 2807.
[19] Y.-H. So, J. P. Heeschen, *J. Org. Chem*. **1997**, *62*, 3552.
[20] Y.-H. So, J. P. Heeschen, B. Bell, P. Bonk, M. Briggs, R. DeCaire, *Macromolecules* **1998**, *31*, 5229.
[21] Y.-H. So, *Acc. Chem. Res*. **2001**, *34*, 753.
[22] J. A. Asensio, S. Borros, P. Gomez-Romero, *J. Electrochem. Soc*. **2004**, *151*, A304.
[23] X. Glipa, B. Bonnet, B. Mula, D. J. Jones, J. Roziere, *J. Mater. Chem*. **1999**, *9*, 3045.
[24] Fuel Cell Handbook (6th Ed.). EG&G Technical Services, Inc. Science Applications International Corporation: **2002**.
[25] B. Xing, O. Savadogo, *J. New Mater. Electrochem. Sys*. **1999**, *2*, 95.
[26] J. R. P. Jayakody, S. H. Chung, L. Durantino, H. Zhang, L. Xiao, B. C. Benicewicz, S. G. Greenbaum, *J. Electrochem. Soc*. **2007**, *154*, B242.
[27] Q. Li, R. He, J.-A. Gao, J. O. Jensen, N. J. Bjerrum, *J. Electrochem. Soc*. **2003**, *150*, A1599.
[28] S. Yu, L. Xiao, B. C. Benicewicz, *Fuel Cells* **2009**, *3-4*, 165.

